

# MCT-1 Oncogene Contributes to Increased *In vivo* Tumorigenicity of MCF7 Cells by Promotion of Angiogenesis and Inhibition of Apoptosis

Anait S. Levenson,<sup>1,2</sup> Kenneth E. Thurn,<sup>1</sup> Laura A. Simons,<sup>1</sup> Dorina Veliceasa,<sup>3</sup> Jennifer Jarrett,<sup>1</sup> Clodia Osipo,<sup>2</sup> V. Craig Jordan,<sup>2,4</sup> Olga V. Volpert,<sup>2,3</sup> Robert L. Satcher, Jr.,<sup>1,2</sup> and Ronald B. Gartenhaus<sup>5</sup>

<sup>1</sup>Department of Orthopaedic Surgery and <sup>2</sup>Robert H. Lurie Comprehensive Cancer Center; <sup>3</sup>Department of Urology, Feinberg School of Medicine, Northwestern University, Chicago, Illinois; <sup>4</sup>Fox Chase Cancer Center, Philadelphia, Pennsylvania; and <sup>5</sup>University of Maryland Greenebaum Cancer Center, Baltimore, Maryland

## Abstract

Overexpression of a novel oncogene MCT-1 (multiple copies in a T cell malignancy) causes malignant transformation of murine fibroblasts. To establish its role in the pathogenesis of breast cancer in humans, we generated stable transfectants of MCF7 breast cancer cells negative for endogenous MCT-1 (MCF7-MCT-1). Overexpression of MCT-1 in these cells resulted in a slight elevation of estrogen receptor- $\alpha$ , and higher rates of DNA synthesis and growth in response to estradiol compared with the empty vector control (MCF7-EV). The pure antiestrogen fulvestrant inhibited the estradiol-stimulated proliferation of MCF7-MCT-1 cells. The MCF7-MCT-1 clones showed increased invasiveness in the presence of 50% serum compared with the MCF7-EV. In a tumor xenograft model, MCT-1-overexpressing cells showed higher take rates and formed significantly larger tumors than MCF7-EV controls. When we examined angiogenic phenotype and molecular mediators of angiogenesis in MCF7-MCT-1 tumors *in vivo*, we found greater microvascular density and lower apoptosis in the MCF7-MCT-1 tumors compared with MCF7-EV controls accompanied by a dramatic decline in the levels of angiogenesis inhibitor, thrombospondin-1 (TSP1). *In vitro*, blocking TSP1 in the medium conditioned by MCT-1-negative cells restored its angiogenic potential to that of the MCF7-MCT-1 cells. Conversely, despite an increase in mRNA encoding vascular endothelial growth factor upon MCT-1 overexpression, vascular endothelial growth factor protein levels have not been notably altered. Taken together, our results suggest that MCT-1 may contribute to the pathogenesis and progression of human breast cancer via at least two routes: promotion of angiogenesis through the decline of TSP1 and inhibition of apoptosis. (Cancer Res 2005; 65(23): 10651-6)

## Introduction

The mechanism of breast cancer progression and metastases is extremely complex. Patients with estrogen receptor (ER)-positive

breast cancers often respond to hormonal therapy and have a better prognosis than patients with ER-negative tumors. The malignant progression of breast tumors is often explained by the transition from the ER-positive to the ER-negative stage; however, the differences in gene expression profiles of breast tumors (1) point to additional factors involved in breast cancer evolution. One approach to understanding the role of such factors in breast cancer genesis and progression is expression of the potentially relevant factor(s) in the ER-positive breast cancer cell lines.

MCT-1 (multiple copies in a T cell malignancy) is a novel candidate oncogene on chromosome Xq22-24, amplified in a T cell lymphoma (2). MCT-1 causes transformation of NIH 3T3 mouse fibroblasts and MCF-10A mammary epithelial cells, shortens their doubling time and G<sub>1</sub> phase of the cell cycle, and is associated with deregulation of the G<sub>1</sub>-S checkpoint and increased expression of cyclin D1 (2-4). MCT-1 stimulates PKB/Akt activation, thus, protecting cells against apoptosis by serum deprivation (5). MCT-1 overexpression has recently been shown in a number of B and T lymphoma cell lines and in a subset of primary diffuse large B cell lymphomas (2, 5).

Here we analyzed MCT-1 expression in breast cancer cells and found higher MCT-1 levels in ER-negative MDA-MB-231, MDA-MB-435, and SK-BR3, whereas ER-positive nonmetastatic MCF7, ZR-75-1, and T47D cells produced none or little MCT-1. This finding has raised the possibility that MCT-1 contributes to the more aggressive metastatic breast cancer phenotype. To verify this hypothesis, we generated stable clones of MCF7 breast cancer cells overexpressing MCT-1 (MCF7-MCT-1) and characterized them *in vitro* and *in vivo*. We found that MCT-1 prompts the transition to a more aggressive phase in breast cancer progression by (a) enhancing invasiveness and decreasing apoptosis, thereby promoting faster growth, and (b) increasing tumor angiogenesis via down-regulation of an endogenous angiogenesis inhibitor, thrombospondin-1 (TSP1). These novel functions of MCT-1, combined with the previously documented protective effect of MCT-1 against stress-induced apoptosis, support its potential role in promoting the progression of breast cancer.

## Materials and Methods

**Cell culture.** The MCF7:WS8 (parental cells), T47D:A18, ZR-75-1, SK-BR3, MDA-MB-231, and MDA-MB-435 cells were maintained in RPMI or MEM with phenol red, 10% fetal bovine serum (FBS), 2 mmol/L L-glutamine, 6 ng/mL bovine insulin, penicillin, and streptomycin. Antiestrogen-resistant MCF7:5C cells were cultured in phenol red-free medium with 5% charcoal-stripped calf serum. Prior to the hormone-sensitive experiments, cells were grown in estrogen-free medium for 3 days before treatment. Estradiol was purchased from Sigma (St. Louis, MO), fulvestrant (ICI 182,780) was a gift from AstraZeneca (Macclesfield, United Kingdom). All the cells were free of *Mycoplasma*.

Note: Supplementary data for this article are available at Cancer Research Online (<http://cancerres.aacrjournals.org/>).

Requests for reprints: Anait S. Levenson, Department of Orthopaedic Surgery, Feinberg School of Medicine, Northwestern University, 645 North Michigan Avenue, S 910, Chicago, IL 60611. Phone: 312-503-3670; Fax: 312-908-8479; E-mail: a-levenson@northwestern.edu or Ronald B. Gartenhaus, The University of Maryland Marlene and Stewart Greenebaum Cancer Center, 9-011 BRB, 655 West Baltimore Street, Baltimore, MD 21201. Phone: 410-328-3691; Fax: 410-328-6559; E-mail: rgartenhaus@som.umaryland.edu.

©2005 American Association for Cancer Research.  
doi:10.1158/0008-5472.CAN-05-0845

**Plasmid constructions and transfections.** MCT-1 coding sequence was amplified from total RNA (Jurkat cells) with the forward 5'-CACCATGTTCAAGAAATTGATGAA-3' and reverse primer 5'-TTTATATGCTTCATATGCCACAGCC-3' and cloned in the TOPO sites of pcDNA3.1/V5-histidine tag vector (Invitrogen, Carlsbad, CA). To subclone into a retroviral vector, the pcDNA3.1-MCT-1-V5-histidine plasmid was again PCR amplified using the primers 5'-TAGAATTCACCATGTTCAAGAAATTGAT-3' and 5'-GGTTAAGCGGGTTTAACTCAAT-3' containing relevant restriction sites (underlined), digested with *EcoRI/HpaI* and ligated into pLXSN (Clontech, Mountain View, CA). The pLXSN-empty vector (EV) and pLXSN-MCT-1-V5-histidine were transfected into PT67 packaging cells, the viral supernatants were collected and added to subconfluent MCF7. After 24 hours, the cells were subjected to selection with 400  $\mu$ g/mL G418 for 2 weeks. Stable clones were evaluated by Western blot for V5-tagged MCT-1 expression.

**Ex vivo cell culture** was established by expansion of tumor cells from two EV-containing and three MCT-1 tumor bearing mice. Fresh tumors were minced with scalpel, smashed under coverslip in six-well tissue culture plate and maintained in the same media as original MCF7-MCT-1 cells.

**Growth assays.** The cells were seeded at 4 to 5  $\times 10^4$  cells/well. The following day, media containing the appropriate compound (estradiol or fulvestrant) were added. The medium was changed every other day for 8 days. The cells were then sonicated and DNA content was measured as described previously (6).

**Western blot analysis.** Western blot analysis was done as described previously (7, 8) using primary antibody for ER- $\alpha$ , TSP1 (NeoMarkers,

Fremont, CA) and MCT-1 (Research Genetics, Huntsville, AL). TSP1 protein levels were examined in conditioned media collected from cell cultures after serum deprivation for 48 to 72 hours. Conditioned medium was concentrated using Amicon ultra filters (Millipore, Bedford, MA). The blots were reprobed for  $\beta$ -actin or stained with Ponceau S to confirm equal loading.

**Invasion assays.** Invasion assays were done using the Cell Invasion Assay kit (Chemicon International, Inc., CA). Briefly, cells (5,000/mL) were maintained in serum-free medium with or without 50% FBS as a chemoattractant at 37°C for 24 hours. Invaded cells were subsequently detached, lysed, and detected by CyQuant GR dye using fluorescence plate reader Mithras LB 940 (Berthold Technologies, Germany).

**Endothelial cell migration assay.** Endothelial cell migration assay was done as described previously (8). Briefly, the cells adhered to one side of the porous membranes were allowed 4 to 6 hours to migrate up the gradient of proangiogenic basic fibroblast growth factor or conditioned medium. The migrated cells were counted in 10 randomly selected fields ( $\times 100$ ). All samples were tested in quadruplicate and each experiment repeated at least twice. ED<sub>50</sub> (50% effective dose) values were determined from the linear regression curves (SigmaPlot software).

**Tumorigenicity assay.** Ovariectomized BALB/c-*nu/nu* 5-week-old athymic mice (5-10 per group) were injected s.c. with 10<sup>6</sup> MCF7-MCT-1 and MCF7-EV cells into axillary mammary fat pads. All animals were implanted with a 0.3 cm silastic estradiol capsules (replaced every 8 weeks). Tumors were measured weekly and tumor areas were calculated as 1/4  $\times$  length  $\times$  width  $\times \pi$ . The data is reported as mean tumor area per group. The tumors

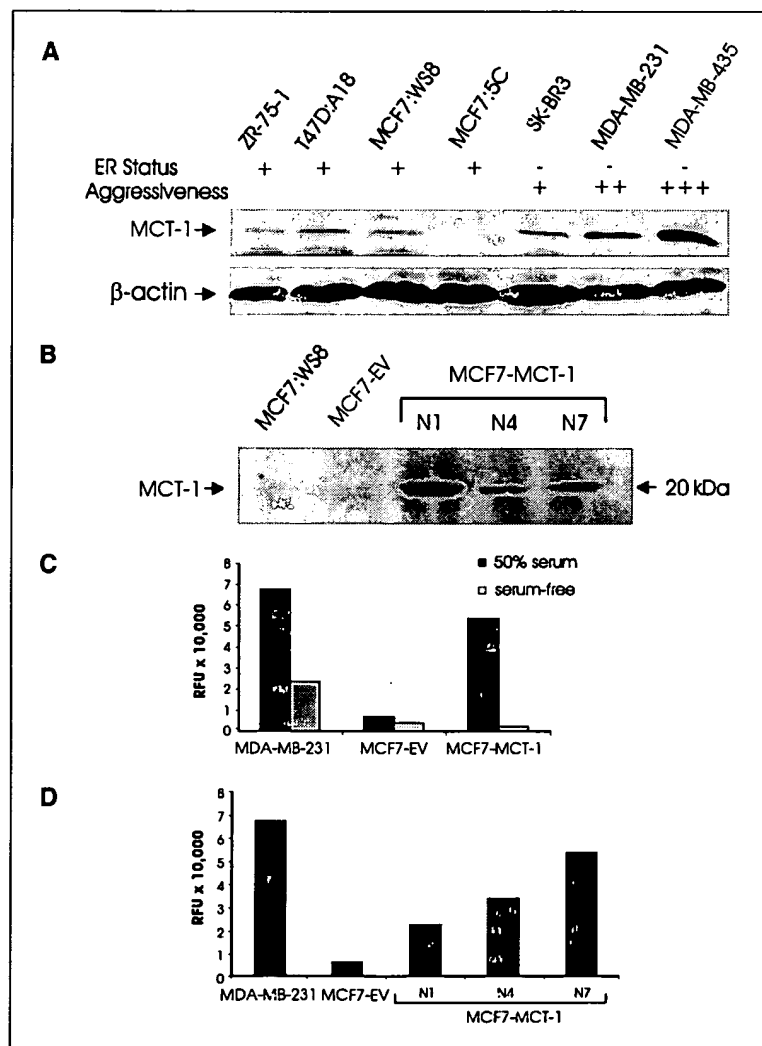


**Figure 1.** A and B, characterization of MCT-1 expression by breast cancer cell lines and stable transfectants. A, Western blot analysis of MCT-1 protein levels in established breast cancer cell lines. ER-positive ZR-75-1, T47D:A18, MCF7:WS8 and ER-negative SK-BR3, MDA-MB-231 and MDA-MB-435 were maintained in estrogenized (phenol red, full serum) RPMI. MCF7:5C cells were cultured in estrogen-free RPMI. B, MCT-1 protein levels in MCF7-MCT-1 stable transfectants. MCF7:WS8, parental cell line; MCF7-EV, vector control; MCF7-MCT-1, MCT-1 expressing clones. C and D, effects of MCT-1 overexpression on the *in vitro* invasion of MCF7 cells. C, highly invasive MCF7-MCT-1 (N7) clone was compared with the MCF7-EV and MDA-MB-231 in 50% FBS and in serum-free medium. Note the lack of invasiveness in the absence of serum. D, invasion of three clones of MCF7-MCT-1 cells in serum-rich medium (50% FBS). Note increased invasiveness of the MCF7-MCT-1 clones compared with MCF7-EV. Experiments were repeated at least five times. Representative experiments are shown. MDA-MB-231 cells were used as a positive control.

were excised and frozen, the lungs and livers were formalin-fixed and paraffin embedded for histologic examination.

**Immunohistochemistry.** To visualize tumor vasculature and TSP1, 5- $\mu$ m-thick sections were simultaneously incubated with TSP1 and CD31

antibody (PharMingen, San Diego, CA) followed by the secondary biotinylated antibody conjugated with Fluorescein Avidin D (VectorLabs, Burlingame, CA) and rhodamine-conjugated antibody (Jackson Immuno-Research, West Grove, PA). Confocal images were captured using a Zeiss LSM510 confocal microscope. CD31-positive structures were counted in 10 randomly chosen fields ( $\times 40$ ), and the average microvascular density was calculated. The intensity of green fluorescence was quantified using ImageJ.

Apoptosis was detected using terminal nucleotidyl transferase-mediated nick end labeling (TUNEL) assay. Vascular endothelial growth factor (VEGF) staining was done at Northwestern University Pathology core. The statistical significance of all numerical data was evaluated using Student's *t* test.

## Results

**Aggressive estrogen receptor-negative breast cancer cells express MCT-1 at higher levels.** To investigate the role of MCT-1 in breast cancer, we analyzed MCT-1 levels in a panel of human breast cancer cells that differ in their aggressiveness and metastatic ability (Fig. 1A). MCF7:WS8, MCF7:5C, and T47D:A18 are all nonaggressive ER $\alpha$ -positive cell lines (9, 10). In contrast, SK-BR3, MDA-MB-231, and MDA-MB-435 cells are ER-negative and highly aggressive and metastatic. As seen in Fig. 1A, MCT-1 was expressed at high levels in the extracts from malignant, ER-negative cells, and at much lower levels in the ER-positive cells.

**Construction of MCT-1 stable transfectants.** We stably transfected MCF7:WS8 cells with pLXSN-EV and pLXSN-MCT1-V5-histidine tag vector and selected three clones with high steady-state levels of MCT-1 (N1, N4, and N7). Western blot analysis showed the bands of expected molecular weight (2) in the cell extracts from MCF7-MCT-1 clones but not from vector controls (Fig. 1B).

**MCF7-MCT-1 cells display increased invasiveness *in vitro*.** As shown in Fig. 1C, in the presence of chemoattractant (50% FBS), MCF7-MCT-1 cells showed significantly increased invasiveness almost reaching the level of MDA-MB-231 cells, whereas the invasiveness of MCF7-EV remained low. The invasiveness varied between the three MCF7-MCT-1 clones in the presence of 50% FBS, however, even the least aggressive N1 clone was considerably more invasive than MCF7-EV control (Fig. 1D).

**MCF7-MCT-1 cells maintain functional estrogen receptor- $\alpha$  and respond to estradiol.** We analyzed ER $\alpha$  protein levels by Western blot (Fig. 2A) and found that MCF7-MCT-1 express ER $\alpha$  at slightly higher levels than the control cells. To further characterize the biological activity of ER $\alpha$  in these cells, we determined the effect of estradiol on ER $\alpha$  protein expression. Consistent with published data (11), we found an estradiol-dependent decrease of ER $\alpha$  protein levels in MCF7-MCT-1 cells and a substantial ER $\alpha$  degradation by fulvestrant (Fig. 2B).

Next, we examined the effect of estradiol and fulvestrant alone and in combination on the growth of MCT-1-overexpressing cells *in vitro*. The ER-positive MCF7-MCT-1 clones showed dose-dependent growth stimulation by estradiol (Fig. 2C). Time-dependent growth analysis with fixed concentrations of estradiol ( $10^{-9}$  mol/L), fulvestrant ( $10^{-6}$  mol/L), or the combination of these two compounds showed strong proliferation in response to estradiol, no effect by fulvestrant alone, and the inhibition of the estradiol-stimulated growth by fulvestrant, further substantiating the functional role of ER $\alpha$  in estradiol-stimulated growth (Fig. 2D). Although MCF7-MCT-1 cells showed a clear trend towards more robust mitogenesis in response to estradiol compared with the MCF7-EV and parental MCF7 cells, the differences were not statistically significant (data not shown).

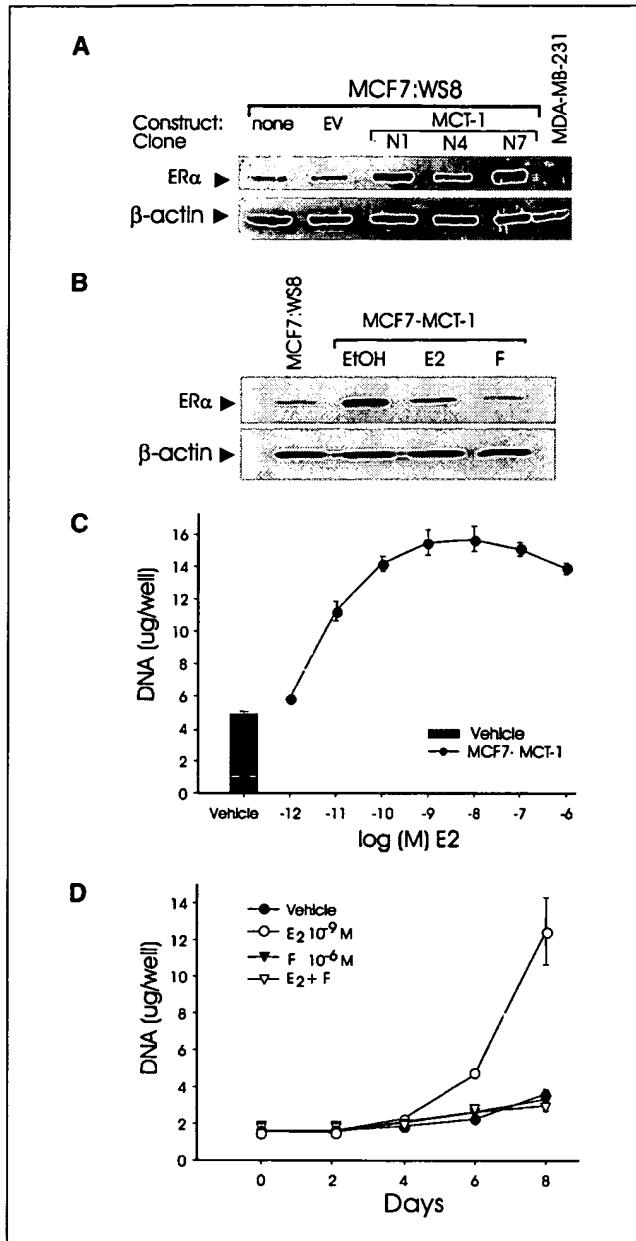


**Figure 2.** A and B, MCF7-MCT-1 cells retained functional ER $\alpha$ . A, ER $\alpha$  protein levels in MCF7-MCT-1 cells were determined by Western blotting. Proteins were resolved on 7.5% SDS-PAGE (20  $\mu$ g cell extract/lane). MCF7:WS8 and MDA-MB-231 cells were used as positive and negative controls, respectively. B, cells treated with ethanol, estradiol ( $10^{-9}$  mol/L), and fulvestrant ( $10^{-6}$  mol/L) for 24 hours were analyzed as in (A). Western blots were repeated at least three times with similar results, representative blots are shown. C and D, dose- and time-estradiol response proliferation of MCF7-MCT1 cells assessed by DNA content. Points, mean of triplicate wells; bars, SE. C, a representative growth curve of N1 clone with varying estradiol concentrations. The cells were maintained in estradiol-free medium and treated with increasing concentrations of estradiol or vehicle (ethanol) for 6 days. D, the inhibition of estradiol-stimulated proliferation of MCF7-MCT-1 by pure antiestrogen fulvestrant (F). The cells were treated for 8 days with ethanol,  $10^{-9}$  mol/L estradiol,  $10^{-6}$  mol/L fulvestrant, or a combination of estradiol and fulvestrant. Each treatment was done in triplicate, the experiment was repeated five times.

**MCT-1 overexpression resulted in increased tumorigenicity.** To test the effect of MCT-1 overexpression on tumorigenicity, two MCT-1-overexpressing MCF7 clones (N1 and N7) as well as MCF7-EV cells, were bilaterally injected into the mammary fat pads of ovariectomized athymic mice in the presence of s.c. estradiol-release pellets. Both MCT-1 transfectants showed higher tumor take at week 7 (37.5% for N1 and 65% for N7) compared with MCF7-EV (20%). At week 14, tumors formed by MCF7-MCT-1 cells were clearly larger than in the control group (Fig. 3A). However, due to the high variability within MCF7-MCT-1 groups and the unexplained mortality, the statistical significance was marginal ( $P < 0.06$  for N1 and  $P < 0.07$  for N7). Nevertheless, at week 17, the surface area of the MCF-MCT-1 tumors was 3.5 to 3.8 times higher than of MCF7-EV tumors (Fig. 3A, right).

We established a new generation of MCT-1 tumors by implanting 1 mm<sup>3</sup> pieces of the MCF7-MCT-1 (N1) and MCF7-EV tumors from the previous experiment, into the mammary fat pads of a new group of mice. The transplanted MCT-1 tumors showed rapid growth and better tumor take than the tumors developed from cell injection. Visible tumors emerged almost immediately in the MCF7-MCT-1 group whereas tumors remained latent for 6 weeks

in the MCF7-EV group (Fig. 3B). By week 11, mean tumor size was significantly greater in the MCF7-MCT-1 (N1) group compared with the MCF7-EV (0.91 and 0.38 cm<sup>2</sup>, respectively;  $P < 0.001$ ; Fig. 3B, right), these differences remained significant ( $P < 0.01$ ) by week 14 despite the diminished group size due to mortality.

Gross and microscopic examination of H&E-stained lung and liver tissues from all tumor-bearing mice revealed no signs of micrometastases (data not shown), suggesting that MCT-1 overexpression alone is insufficient to promote spontaneous dissemination of MCF7 cells.

**MCF7-MCT-1 tumors were more vascularized and less apoptotic than control MCF7-EV tumors.** Histologic analysis revealed low cellular density and sizeable necrotic areas for MCF7-EV and a "healthy" appearance for MCF7-MCT-1 tumors (Fig. 4A, H&E). Moreover, MCF7-MCT-1 tumors showed significant, 2.6-fold reduction of apoptosis (Fig. 4A and B, TUNEL;  $P < 0.0000000001$ ) compared with the control. Such central necrotic areas and high apoptotic rates are likely to emerge from poor vascularization and resulting hypoxia. We, therefore, compared the microvascular densities of MCF7-MCT-1 and MCF7-EV tumors at week 14.

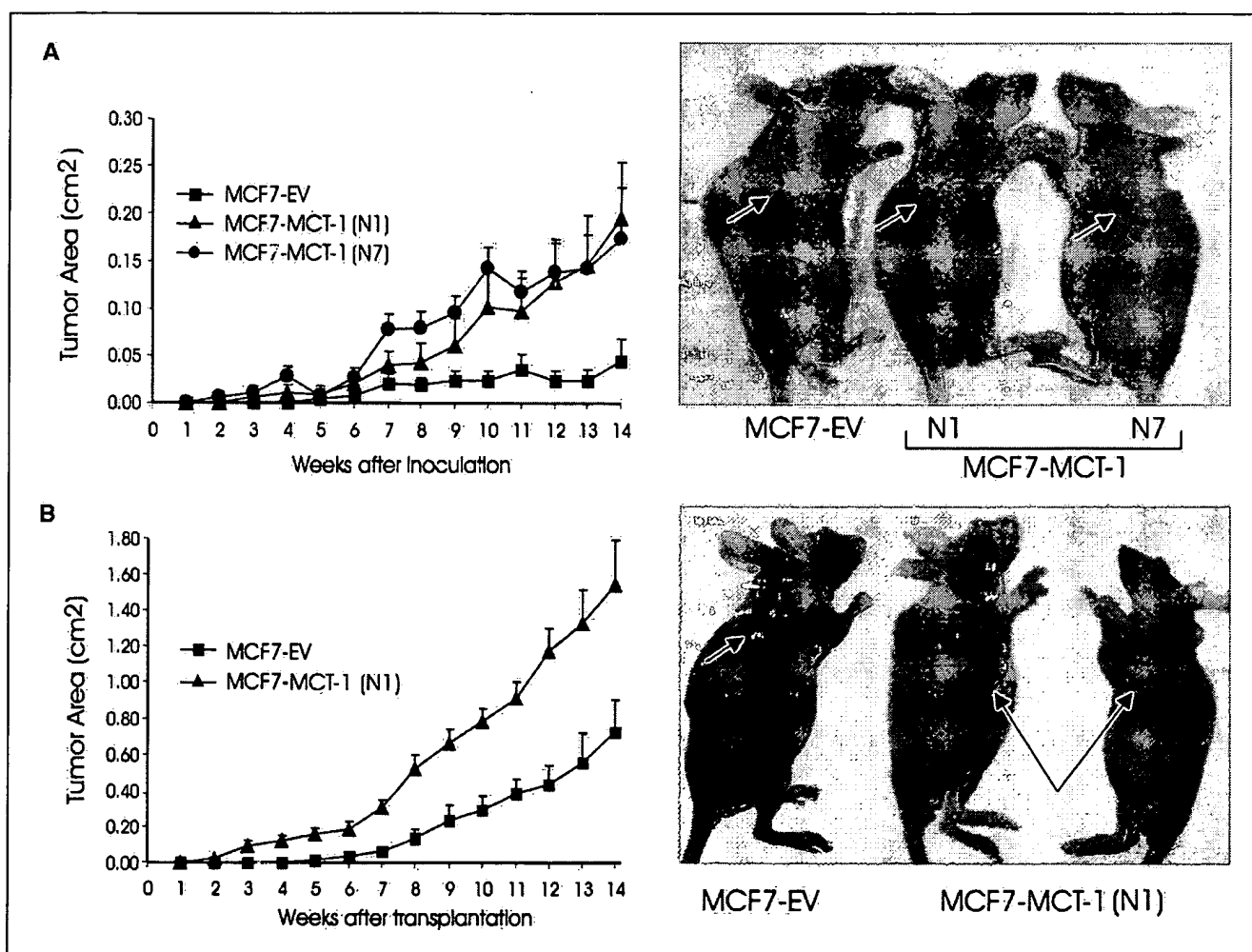
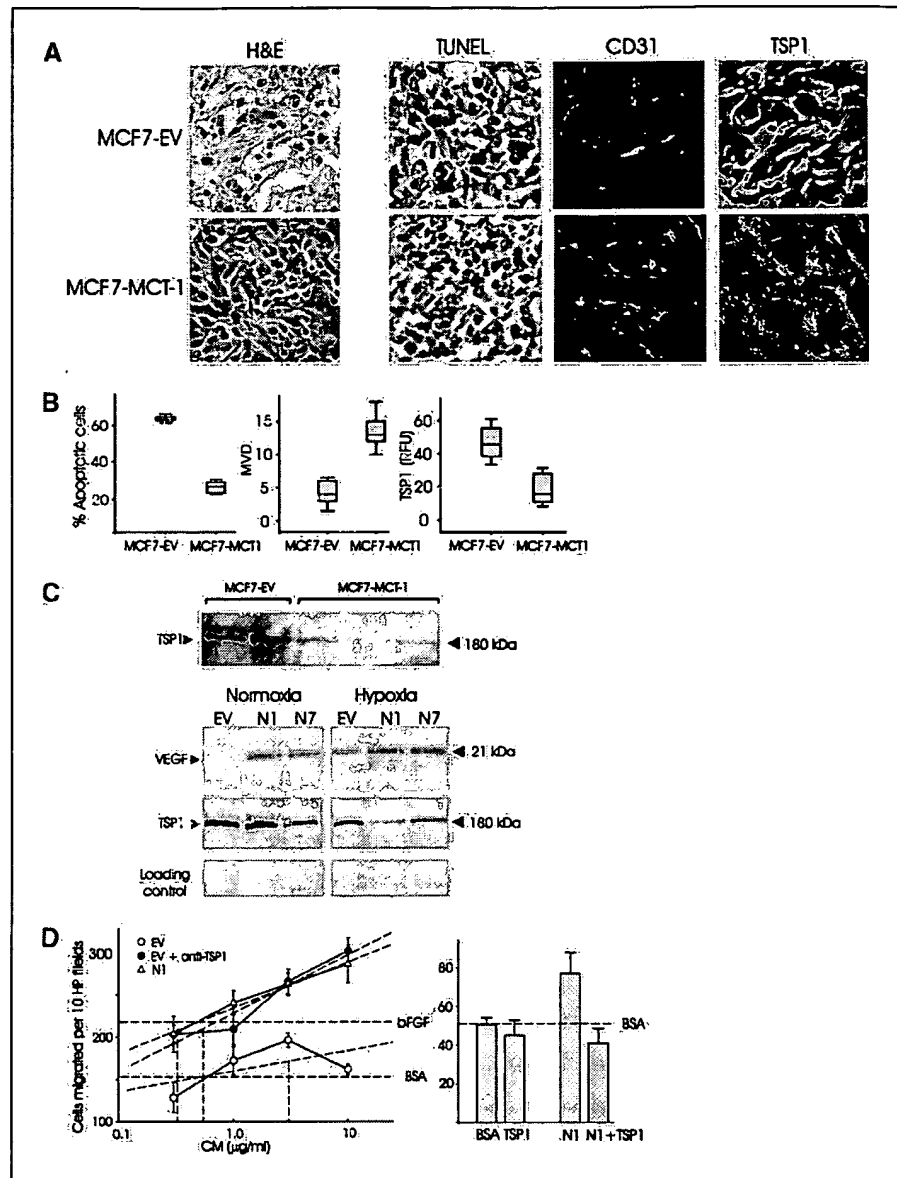


**Figure 3.** A, increased tumorigenicity of MCT-1 overexpressing MCF7 cells. MCF7-MCT-1 (N1 and N7) and MCF7-EV cells were inoculated into mammary fat pads of ovariectomized athymic mice implanted with estradiol pellets. *Left*, tumor growth curves; (▲) N1, (●) 7, and (■) MCF7-EV. *Right*, tumor-bearing mice representative of each group at 17 weeks, arrows point at tumors. B, tumor progression in mice bearing implanted fragments from MCF7-EV and MCT-1 (N1) tumors from experiment shown in (A). *Left*, tumor growth curves. Note larger tumor sizes and significant differences between groups starting at week 8 ( $P < 0.001$ ). *Right*, representative mice from each group at week 14 after implantation.

**Figure 4.** Increased vascularization of the tumors overexpressing MCT-1 correlated with reduced TSP1 expression. **A**, histologic and morphologic characteristics of control and MCT-1 tumor (H&E staining). Note the decreased cellular density with large necrotic areas in the MCF7-EV compared with healthy-looking cells and fibrotic areas in MCF7-MCT-1 tumor. **TUNEL**, tumor cell apoptosis of MCF7-MCT-1 and MCF7-EV tumors determined by *in situ* TUNEL analysis of tumor sections (brown, TUNEL-positive nuclei) was quantified by manual count and the percentage of apoptotic cells per high-powered field was calculated (**B**;  $P < 0.0000000001$ ). **CD31**, tumor sections were stained with antibodies against endothelial marker, CD31 (red immunofluorescence) and quantitative analysis of vascularization were done (**B**, the number of CD31-positive structures per high-powered  $\times 40$  field;  $P < 0.0000002$ ). **TSP1**, increased vascularization in MCF7-MCT-1 tumors was concomitant with reduced TSP1 expression (green immunofluorescence). **B**, quantitative analysis of immunofluorescence ( $P < 0.00000013$ ). RFU, relative fluorescence units. **C**, effect of MCT-1 overexpression on angiogenic phenotype *in vitro*. **Top**, *ex vivo* cultures expanded from MCF7-EV tumors ( $n = 2$ ) expressed much higher amounts of TSP1 compared with *ex vivo* cultures from MCF7-MCT-1 tumors ( $n = 3$ ). Conditioned media were collected as described in Materials and Methods and subjected to Western blotting with anti-TSP1 antibody. **Bottom**, in hypoxia, levels of TSP1 secreted by MCF7-MCT-1 conditioned medium were significantly lower than in MCF7-EV conditioned medium. In contrast, VEGF levels were increased. Conditioned medium was collected from cells maintained in hypoxia chamber (1.5%  $O_2$ ; Coy Instruments, Grass Lake, MI) for 48 hours and subjected to Western blotting with anti-VEGF and anti-TSP1 antibody. **D**, overexpression of MCT-1 enhanced proangiogenic phenotype via suppression of TSP1. **Left**, serum-free medium were tested for the ability to promote the migration of cells in the absence ( $\circ$ ) and in the presence ( $\bullet$ ) of neutralizing TSP1 antibody. **Right**, TSP1 peptide ABT10 (100 nmol/L) completely blocked the ability of MCF7-MCT-1 conditioned medium (N1, 10  $\mu$ g/mL) to stimulate endothelial cell chemotaxis. **Horizontal dotted lines**, background migration (BSA), and migration stimulated by basic fibroblast growth factor (bFGF; 10 ng/mL). **Points**, means; **bars**, SE.



Indeed, MCT-1 overexpression resulted in a dramatic  $\sim 3.5$ -fold increase in the median tumor microvascular density (Fig. 4A and B, CD31;  $P < 0.00000015$ ).

**MCT-1 overexpression caused a decrease in the angiogenesis inhibitor, thrombospondin-1.** Seeking a mechanism behind the proangiogenic effect of MCT-1, we examined two angiogenic factors critical in breast cancer, proangiogenic VEGF and antiangiogenic TSP1 (12). Immunostaining revealed relatively high VEGF levels, typical for breast cancer, with no significant differences between MCF7-MCT-1 and MCF7-EV tumors (data not shown). In contrast, *in situ* immunofluorescence showed striking differences in the levels of natural angiogenesis inhibitor, TSP1, with  $\sim 3$ -fold reduction of the TSP1 expression in the MCF7-MCT-1 tumors compared with the MCF7-EV control (Fig. 4A and B, TSP1;  $P < 0.00000013$ ). Therefore, it is likely that increased vascularization of MCF7-MCT-1 tumors stems from the decline of inhibitory TSP1.

To confirm the role of TSP1, we measured TSP1 mRNA and protein levels in tumors, *ex vivo* cell cultures, and original cell lines.

Semiquantitative RT-PCR showed lower TSP1 mRNA levels in MCF7-MCT-1 tumors compared with the MCF7-EV tumors (data not shown; Supplementary data; Fig. 5). Interestingly, VEGF mRNA was higher in MCT-1 tumors compared with vector controls. Western blot analysis of *ex vivo* cultures showed higher levels of TSP1 secreted by MCF7-EV tumor cells compared with MCF7-MCT-1 (Fig. 4C, top). When conditioned medium was collected under hypoxia (1.5%  $O_2$ ), to mimic the *in vivo* tumor environment, VEGF levels became similar in both EV- and MCT-1-expressing cells. In contrast, TSP1 levels were dramatically lower in MCF7-MCT-1 conditioned medium compared with MCF7-EV (Fig. 4C, bottom). To determine the functional consequences of the MCT-1-driven decline of TSP1, we measured endothelial cell chemotaxis in the presence of conditioned medium from the cells collected in hypoxia. The secretions of the MCT-1 expressing cells were more angiogenic as was reflected by their lower  $ED_{50}$  values (0.3 versus 2.9  $\mu$ g/mL for EV). Adding TSP1-neutralizing antibodies restored the migratory capability of MCF7-EV cells ( $ED_{50} \approx 0.7$   $\mu$ g/mL; Fig. 4D, left),

whereas isotype control IgA had no effect (data not shown). In contrast, TSP1 active antiangiogenic peptide ABT-510 (13) completely blocked the ability of conditioned medium from MCF7-MCT-1 cells to stimulate endothelial cell chemotaxis (Fig. 4D, right).

## Discussion

The fact that MCT-1 was expressed at high levels in the aggressive breast cancer cells prompted us to examine its potential role in breast cancer progression. Like parental cells, MCF7-MCT-1 retained functional ER- $\alpha$  and estradiol-responsiveness, however, they gained enhanced ability to invade *in vitro*, further supporting the role of MCT-1 in increasing metastatic potential (2).

Although MCF7-MCT-1 and MCF7-EV grew at a similar rate in culture, in nude mice, MCF7-MCT-1 formed estradiol-dependent tumors much faster, especially when previously established tumors were transplanted to a new group of mice. Thus, we have shown for the first time that MCT-1 overexpression in MCF7 breast cancer cells results in a higher rate of tumor progression. Despite enhanced invasiveness of MCF7-MCT-1 cells, MCT-1 was insufficient to cause MCF7-MCT-1 tumors to metastasize, suggesting the requirement for additional factors.

The lack of differences between the growth rates *in vitro* combined with considerably increased tumorigenicity *in vivo* suggested a possible role for MCT-1 in the regulation of tumor angiogenesis. This hypothesis was corroborated by a dramatic 2.7-fold increase in the vascularity of the MCT-1-positive tumors. The MCT-1-driven increase in angiogenesis coincided with an extensive decrease of tumor cell apoptosis, which explains, at least in part, the accelerated growth of MCF7-MCT-1 tumors. Moreover, central necrotic areas characteristic of hypoxia due to insufficient vascularization (14) were present in all MCT-1-negative tumors and were absent in the MCF7-MCT-1 tumors.

Tumor angiogenesis is determined by the balance between extracellular mediators of angiogenesis, increased expression of the proangiogenic molecules (inducers), or decrease in the secreted inhibitor(s) (12), which in turn might be controlled by the loss of tumor suppressors and the activation of oncogenes (15). Here, we established that the MCT-1 oncogene participates in angiogenic switch in MCF7 breast cancer cells *in vitro* and *in vivo*.

Several mediators of angiogenesis have been linked to breast cancer progression. Of the inducers, VEGF is the most prominent:

its overexpression promotes local tumor growth and brain metastases in the mouse model of breast cancer (16). Conversely, the angiogenic switch may occur due to the loss of potent inhibitor, TSP1, which is expressed at high levels in normal breast tissue. Higher TSP1 levels in the stroma around ductal carcinoma *in situ* indicate favorable prognoses (17), moreover, forced TSP1 expression reverses the angiogenic switch and reduces tumorigenicity (18).

In our estrogen-dependent breast cancer model, MCT-1 overexpression severely decreased the levels of TSP1 mRNA and protein, suggesting that MCT-1 causes angiogenic switch predominantly by suppressing inhibitory TSP1. Indeed, by neutralizing TSP1, we were able to restore the angiogenic activity of the MCF7-EV cells to the levels close to those of MCF7-MCT-1, whereas exogenous TSP1 blocked angiogenesis by MCF7-MCT1. Interestingly, the changes in TSP1 expression could only be registered under hypoxic conditions, suggesting that MCT-1 may suppress TSP1 via one of the hypoxia-inducible transcription factors (15). Conversely, MCT-1 overexpression resulted in constitutively high VEGF levels, even in high oxygen content, whereas hypoxia caused increased VEGF secretion by MCF7-EV, thus, muffling the differences in VEGF as was registered by immunostaining.

In summary, this is the first study to show the role of MCT-1 in breast cancer. Our observations suggest a new function for MCT-1, the control of angiogenic phenotype via down-regulation of the antiangiogenic protein, TSP1. In addition, MCT-1 overexpression inhibited tumor apoptosis. Taken together with documented proliferative and antiapoptotic roles of MCT-1 (2, 3, 5), our observations support a role for MCT-1 in the progression of breast cancer towards aggressive, highly vascularized tumors.

## Acknowledgments

Received 3/14/2005; revised 9/15/2005; accepted 9/27/2005.

**Grant support:** Pilot grant from the Specialized Programs of Research Excellence (CA89018-01) and a pilot grant from the AVON Foundation (A.S. Levenson), A Merit Review Award from the Department of Veterans Affairs and a pilot grant from the AVON Foundation (R.B. Gartenhaus), and NIH grant RO1 HL68003-04 (D. Veliceasa and O.V. Volpert).

The costs of publication of this article were defrayed in part by the payment of page charges. This article must therefore be hereby marked *advertisement* in accordance with 18 U.S.C. Section 1734 solely to indicate this fact.

We are grateful to Dr. Kidwai and the Pathology Core of Northwestern University for TUNEL, VEGF, and H&E stainings; Antonio J. Quesada (Universidad Autonoma, Madrid, Spain) for the measurements of TSP1 immunofluorescence; and Dr. J Wang for helpful discussions.

## References

- Perou CM, Sorlie T, Eisen MB, et al. Molecular portraits of human breast tumours. *Nature* 2000;406:747-52.
- Prosniak M, Dierov J, Okami K, et al. A novel candidate oncogene, MCT-1, is involved in cell cycle progression. *Cancer Res* 1998;58:4233-7.
- Dierov J, Prosniak M, Gallia G, Gartenhaus RB. Increased G<sub>1</sub> cyclin/cdk activity in cells overexpressing the candidate oncogene, MCT-1. *J Cell Biochem* 1999;74:544-50.
- Hsu HL, Shi B, Gartenhaus RB. The MCT-1 oncogene product impairs cell cycle checkpoint control and transforms human mammary epithelial cells. *Oncogene* 2005;24:4956-64.
- Shi B, Hsu HL, Evens AM, Gordon LI, Gartenhaus RB. Expression of the candidate MCT-1 oncogene in B- and T-cell lymphoid malignancies. *Blood* 2003;102:297-302.
- Levenson AS, Kwaan HC, Svoboda KM, Weiss IM, Sakurai S, Jordan VC. Estradiol regulation of components of the plasminogen-plasmin system in MDA-MB-231 human breast cancer cells stably expressing the estrogen receptor. *Br J Cancer* 1998;77:1812-9.
- Levenson AS, Gehm BD, Timm Pearce S, et al. Resveratrol acts as an estrogen receptor (ER) agonist in breast cancer cells stably transfected with ER $\alpha$ . *Int J Cancer* 2003;104:587-96.
- Volpert OV, Dameron KM, Bouck N. Sequential development of an angiogenic phenotype by human fibroblasts progressing to tumorigenicity. *Oncogene* 1997;14:1495-502.
- Jiang S-Y, Wolf DM, Yingling JM, Chang C, Jordan VC. An estrogen receptor positive MCF-7 clone that is resistant to antiestrogens and estradiol. *Mol Cell Endocrinol* 1992;90:77-86.
- Murphy CS, Pink JJ, Jordan VC. Characterization of a receptor-negative, hormone-nonresponsive clone derived from T47D human breast cancer cell line kept under estrogen-free conditions. *Cancer Res* 1990;50:7285-92.
- Pink JJ, Jordan VC. Models of estrogen receptor regulation by estrogens and antiestrogens in breast cancer cell lines. *Cancer Res* 1996;56:2321-30.
- Hanahan D, Folkman J. Patterns and emerging mechanisms of the angiogenic switch during tumorigenesis. *Cell* 1996;86:353-64.
- Reiher FK, Volpert OV, Jimenez B, et al. Inhibition of tumor growth by systemic treatment with thrombospondin-1 peptide mimetics. *Int J Cancer* 2002;98:682-9.
- Carmeliet P, Dor Y, Herbert JM, et al. Role of HIF-1 $\alpha$  in hypoxia-mediated apoptosis, cell proliferation and tumour angiogenesis. *Nature* 1998;394:485-90.
- Jimenez B, Volpert OV. Mechanistic insights on the inhibition of tumor angiogenesis. *J Mol Med* 2001;78:663-72.
- Kim LS, Huang S, Lu W, Lev DC, Price JE. Vascular endothelial growth factor expression promotes the growth of breast cancer brain metastases in nude mice. *Clin Exp Metastasis* 2004;21:107-18.
- Rice AJ, Steward MA, Quinn CM. Thrombospondin 1 protein expression relates to good prognostic indices in ductal carcinoma *in situ* of the breast. *J Clin Pathol* 2002;55:921-5.
- Weinstat-Saslow DL, Zabrenetzky VS, VanHoutte K, Frazier WA, Roberts DD. Transfection of thrombospondin 1 complementary DNA into a human breast carcinoma cell line reduces primary tumor growth, metastatic potential, and angiogenesis. *Cancer Res* 1994;54:6504-11.

# Expression of the candidate *MCT-1* oncogene in B- and T-cell lymphoid malignancies

Bo Shi, Hsin-Ling Hsu, Andy M. Evens, Leo I. Gordon, and Ronald B. Gartenhaus

Our laboratory has recently discovered a novel candidate oncogene, *MCT-1*, amplified in human T-cell lymphoma and mapped to chromosome Xq22-24. This region is amplified in a subset of primary B-cell non-Hodgkin lymphoma (NHL), suggesting that increased copy number of a gene(s) located in this region confers a growth advantage to some primary human lymphomas. We examined a diverse panel of lymphoid malignancies for the expression of *MCT-1*. We demonstrated that there are significantly increased levels of *MCT-1* protein in a panel of T-cell lymphoid cell lines and in non-Hodgkin

lymphoma cell lines. Furthermore, we identified a subset of primary diffuse large B-cell lymphomas that exhibited elevated levels of *MCT-1* protein. Interestingly, all transformed follicular lymphomas in our study demonstrated elevated protein levels of *MCT-1*. There was no detectable *MCT-1* protein in leukemic cells from patients with chronic lymphocytic leukemia or in any healthy lymphoid tissue examined. Lymphoid cell lines overexpressing *MCT-1* exhibited increased growth rates and displayed increased protection against apoptosis induced by serum starvation when compared with matched con-

trols. We found that *MCT-1*-overexpressing cells show constitutively higher levels of phosphorylated PKB/Akt protein, especially under serum starvation. Activation of survival pathways may be an additional function of the *MCT-1* gene. Our data suggest that high levels of *MCT-1* protein may be associated with a high-risk subset of lymphoid neoplasms and may further support the potential role of *MCT-1* in promoting human lymphoid tumor development. (Blood. 2003;102:297-302)

© 2003 by The American Society of Hematology

## Introduction

Random genomic instability, as seen in many epithelial cancers, is not a characteristic of the more stable lymphoma genome. Furthermore, defects in DNA-mismatch repair that manifest as genomic microsatellite instability, commonly found in various hereditary solid tumor syndromes, and rare sporadic cancers are less recognized in lymphoma.<sup>1,2</sup> Genetic alterations frequently identified in lymphomagenesis include chromosome rearrangements, disruption of tumor-suppressor genes, and increase in copy number of genes (gene amplification). We have previously identified an amplified DNA sequence in the Hut 78 T-cell lymphoma cell line that was subsequently shown to represent a novel candidate oncogene mapped to chromosome Xq22-24.<sup>3</sup> This region is amplified in a subset of primary B-cell non-Hodgkin lymphoma (NHL),<sup>4,6</sup> suggesting that increased copy number of a gene(s) located in this region confers a growth advantage to a subset of primary human lymphomas. Recently, analysis of the cell-cycle regulation of *MCT-1* protein levels displayed little variation of *MCT-1* protein during the cell-cycle progression.<sup>7</sup> However, levels of *MCT-1* protein are rapidly induced in irradiated human lymphoid cells through a posttranslational mechanism,<sup>7</sup> consistent with *MCT-1* as a DNA damage-response gene. In this report, we examined the expression profile of *MCT-1* protein along a spectrum of human lymphoid tumors. Our results demonstrated that *MCT-1* protein expression was elevated in some samples of aggressive lymphoma, including diffuse large B-cell lymphoma (DLBCL) and interleukin-2 (IL-2)-independent T-cell lymphoid tumors. Moreover, we

also observed that *MCT-1* expression levels are strongly associated with the cell proliferation marker, proliferating cell nuclear antigen (PCNA). In addition, lymphoid cells that are stably transfected with an *MCT-1* retroviral construct exhibited increased proliferative rates and increased protection against apoptosis induced by serum starvation when compared with matched controls. These data suggest that high levels of *MCT-1* protein may be associated with a high-risk subset of lymphoid neoplasms and support a possible role for *MCT-1* in human lymphomagenesis.

## Patients, materials, and methods

### Cell lines, healthy tissues, and tumor specimens

Six T-cell lines, 3 which are IL-2 dependent—EC155 (Advanced Biotechnologies, Columbia, MD) N1185,<sup>8</sup> and N1186<sup>8</sup>—and 3 which are IL-2 independent—Hut 78, MT-2, and Jurkat (Advanced Biotechnologies)—and 7 NHL cell lines—SU-DHL-4, SU-DHL-6, SU-DHL-7, SU-DHL-8, SU-DHL-10, Namalwa, and Ly3 (ATCC, Manassas, VA)—were chosen for this study. All T-cell lines were cultured in complete RPMI 1640 with 40 U/mL recombinant IL-2 (Invitrogen, Carlsbad, CA) added to the IL-2-dependent lines. Healthy donor peripheral blood lymphocytes (PBL) were isolated by centrifugation over Ficoll-Hypaque as previously described<sup>9</sup> (Pharmacia, Pleasant Hill, CA). After phytohemagglutinin (PHA) stimulation, these lymphocytes were cultured in a manner similar to that for IL-2-dependent T-cell lines, as described. Leukemic cells from patients with chronic lymphocytic leukemia (CLL) were obtained, after informed consent was

From the Division of Hematology/Oncology, Department of Medicine, Northwestern University Feinberg School of Medicine, and the Robert H. Lurie Comprehensive Cancer Center, Northwestern University, Chicago, IL.

Submitted November 19, 2002; accepted February 28, 2003. Prepublished online as Blood First Edition Paper, March 13, 2003; DOI 10.1182/blood-2002-11-3486.

Reprints: Ronald B. Gartenhaus, Division of Hematology/Oncology,

Department of Medicine, Northwestern University Feinberg School of Medicine, 303 E Chicago Ave, Chicago, IL 60611; e-mail: r-gartenhaus@northwestern.edu.

The publication costs of this article were defrayed in part by page charge payment. Therefore, and solely to indicate this fact, this article is hereby marked "advertisement" in accordance with 18 U.S.C. section 1734.

© 2003 by The American Society of Hematology

given, by Ficoll-Hypaque centrifugation (Pharmacia). White blood counts ranged from 10,000 to 90,000  $\mu\text{L}$ , with more than 80% lymphocytes in all samples. No patient had been exposed to chemotherapy for at least 3 months before sampling. Lymph node biopsy specimens from patients with primary DLBCL and normal lymph nodes were used in this study. All primary tumor samples examined were obtained at diagnosis before treatment and were stored as fresh-frozen biopsy specimens and preserved at  $-80^{\circ}\text{C}$  in the Pathology Core Laboratory of the Robert H. Lurie Comprehensive Cancer Center at Northwestern University Feinberg School of Medicine. Approval was obtained from the Northwestern University institutional review board for these studies. Informed consent was provided according to the Declaration of Helsinki.

### Western blot analysis

Cell lines ( $2 \times 10^7$  cells) were washed twice in phosphate-buffered saline (PBS), lysed in 300  $\mu\text{L}$  RIPA buffer containing 20  $\mu\text{L}$  protease inhibitor cocktail (Sigma, St Louis, MO), and incubated on ice for 30 minutes. Primary frozen tumor tissue samples were homogenized with Dounce homogenizers in RIPA buffer. Samples from cell lines and tissues were further disrupted by passage through 21-gauge needles. The supernatant fluid of total cell lysate was taken after 10 000g centrifugation for 10 minutes. In general, 40  $\mu\text{g}$  protein was separated on 10% sodium dodecyl sulfate–polyacrylamide gel electrophoresis (SDS-PAGE) at room temperature. The proteins were transferred to Hybond nitrocellulose membrane (Amersham Pharmacia Biotech, Buckinghamshire, United Kingdom) with the use of a semidry electroblotter (Bio-Rad, Hercules, CA). Membranes were blocked in 5% nonfat milk Tris-buffered saline–Tween (TBST) and subsequently were incubated with the following primary antibodies: rabbit polyclonal antihuman MCT-1 (Research Genetics, Huntsville, AL), mouse monoclonal antihuman  $\beta$ -actin (Sigma), mouse monoclonal antihuman PCNA (Santa Cruz Biochemicals, Santa Cruz, CA), mouse monoclonal anti-V5 (Invitrogen), rabbit polyclonal anti-phospho-AKT (Ser473) (Cell Signaling, Beverly, MA), goat polyclonal anti-AKT (Cell Signaling), and a horseradish peroxidase (HRP)–conjugated secondary antibody. Specific proteins were detected by enhanced chemiluminescence (ECL; Amersham) and film exposure.

### RT-PCR SSCP analysis for mutation detection

Reverse transcription–polymerase chain reaction (RT-PCR) was performed for single-strand conformational polymorphism (SSCP). PCR primer sets used for the 5' end portion of MCT-1 were: forward, AACCGTTGCCTAAAGGAG; reverse, TGTTTCATGGCATCGGACTATTT (product of 410bp). PCR primer sets used for the 3' end portion of MCT-1 were: forward, AAATAGTCCGATGCCATGAACA; reverse, ACACAGACACAAACAGATACAG (product of 465 bp). PCR cycling was carried out as follows:  $94^{\circ}\text{C}$  for 1 minute followed by 34 cycles of denaturation at  $94^{\circ}\text{C}$  for 1 minute, annealing at  $58^{\circ}\text{C}$  for 45 seconds, extension at  $72^{\circ}\text{C}$  for 1 minute; final chain elongation at  $72^{\circ}\text{C}$  for 5 minutes. Ten-microliter PCR product mixed with 2  $\mu\text{L}$  10  $\times$  Blue Juice loading buffer (Gibco, Carlsbad, CA) was denatured at  $95^{\circ}\text{C}$  for 4 minutes and then made ice cold for 2 minutes. The mixture was separated by 6% polyacrylamide/5% glycerol gel and was silver stained according to the procedures described.<sup>10</sup> The gel was dried at  $80^{\circ}\text{C}$  for 30 minutes and then scanned into a computer by a Microtek Scanner.

### Establishment of stable MCT-1 overexpressing lymphoid cell line

The cDNA fragment containing the coding region of MCT-1 was amplified by RT-PCR using total RNA from healthy donor PBL cells. This sequence was subcloned into the TOPO cloning site of pcDNA3.1/V5-Histidine tag vector (Invitrogen). The pcDNA3.1-MCT-1-V5 plasmid was extracted from the vector and used to transform Top 10 bacteria (Invitrogen). The new sequence containing the MCT-1 coding region was fused with a V5-histidine tag in C-terminal and was PCR amplified from pcDNA3.1-MCT-1-V5 plasmid by the forward primer of 5'-TAGAATTCACCATGTTCAA-GAAATTTGAT-3' and reverse primer 5'-GGTTAACAGCGGGTTTA-

AACTCAAT-3'. This fragment was then digested with *EcoRI* and *HpaI* and was ligated to the *EcoRI* and *HpaI* sites of the retroviral expression vector pLXSN (Clontech, Palo Alto, CA). pLXSN vector or pLXSN-MCT-1-V5 vector was transfected into the packaging cell line, PT67, and recombinant retroviral RNAs were packaged into infectious, replication-incompetent particles. Culture media containing viral particles were collected. Viral-containing medium was added to the EC155 cell culture medium. Infected EC155 cells were selected after growing in 10% serum RPMI 1640 supplemented with 300  $\mu\text{g}/\text{mL}$  geneticin (G418) for 3 weeks. Individual clones of stably infected cells with pLXSN vector or pLXSN-MCT-1-V5 were obtained by limiting dilution. The following independently isolated clones were used for our experiments: EC155-Vector,<sup>4</sup> EC155-Vector,<sup>5</sup> EC155-MCT-1,<sup>4</sup> EC155-MCT-1,<sup>5</sup> and EC155-MCT-1.<sup>7</sup>

### Confocal Immunofluorescence

EC155-Vector and EC155-MCT-1 cells were washed once with PBS in 15-mL tubes. Cells were fixed in 2 mL absolute methanol for 5 minutes at room temperature (RT). After fixation, cells were washed with 5 mL PBS 3 times. Cells were incubated in 2 mL block solution (PBS containing 10% fetal bovine serum) for 20 minutes at RT. The block solution was replaced by 0.5 mL PBS–10% containing primary antibody, mouse monoclonal anti-V5 (1:250 dilution; Invitrogen), or mouse monoclonal anti-PCNA (1:500; Santa Cruz Biotechnology). Cells were incubated with primary antibody at  $40^{\circ}\text{C}$  overnight. Then cells were washed 3 times with 5 mL PBS and were incubated with 0.5 mL PBS–10% containing the secondary antibody, anti-mouse immunoglobulin G2a (IgG2a)–fluorescein (1:250 dilution; Roche Molecular Biochemicals, Mannheim, Germany) for 2 hours. After 3 washes with PBS, the cells were spread on slides and mounted on a coverglass with mounting medium. The slides were then viewed using a Zeiss LSM510 confocal scanning laser microscope (Oberkochen, Germany). Green fluorescence was detected using an excitation of 395 nm and an emission of 505 nm. Fluorescence images were saved on a computer, and the results were printed out on a Fujix Pictography 3000 digital printer.

### Cell growth, viability, and apoptosis assays

Cell lines used were either EC155-Vector or EC155-MCT-1 clones. Cell lines were cultured in RPMI 1640 (Life Technologies, Gaithersburg, MD) supplemented with 10% fetal calf serum (FCS; Life Technologies) and 40 U/mL recombinant IL-2 (Life Technologies).

EC155-Vector or EC155-MCT-1 was seeded at  $0.5 \times 10^6$  cells/mL in triplicate T-25 flasks with 10 mL complete RPMI 1640 supplemented with 40 U/mL recombinant IL-2. IL-2 was replenished every 3 days. Cells were counted every other day for 8 days, and viability was measured using the trypan blue exclusion method. Mean cell number and its standard deviation for each time point were calculated using standard methodology as previously performed.<sup>3</sup>

To investigate a possible role of MCT-1 in cell survival, the effect of serum deprivation was investigated. We seeded  $2 \times 10^6$  cells/mL of either EC155-Vector or EC155-MCT-1 clones in duplicate T-25 flasks with serum-reduced culture medium that contained 0.2% FCS and 40 U/mL IL-2 in RPMI 1640 medium. After 24, 48, and 72 hours of culture, cell viabilities of both cell lines were analyzed using the trypan blue dye exclusion method.

To determine whether cell death was caused by apoptosis, annexin V binding assays and mitochondrial membrane potential (MMP) assays were performed. We used an immunofluorescence assay to simultaneously detect MMP and annexin V binding of the cells. In brief, cell pellets were collected and resuspended with culture medium to reach a final cell concentration of  $1 \times 10^6$  cells/mL. Fifty microliters CMX Rosamine (Beckman Coulter, Brea, CA) was added to 0.5 mL cell suspension and vortexed gently. Cell-containing tubes were placed in a  $\text{CO}_2$  incubator at  $37^{\circ}\text{C}$  for 15 minutes. Each tube containing 1 mL PBS was spun at 1200 rpm for 5 minutes. Supernatant was discarded, and cells were resuspended in 500  $\mu\text{L}$  cold 1  $\times$  binding buffer from the annexin V-FITC kit (Beckman Coulter). Five microliters annexin V-FITC was added to the cell suspension, and the tube was vortexed gently and put at  $40^{\circ}\text{C}$  for 10 minutes. Stained cells were immediately analyzed by flow cytometry.

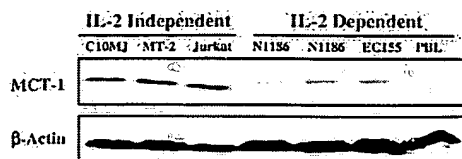


**Figure 1.** Steady-state MCT-1 protein levels in exponentially growing T-lymphoid cell lines. Forty micrograms total proteins from IL-2-dependent cell lines PBL, EC155, N1185, and N1186, and IL-2-independent cell lines C10MJ, MT-2, and Jurkat were subjected to SDS-PAGE analysis and blotted on the membrane. Western blotting was performed with MCT-1 polyclonal antibody. Control immunoblotting was carried out with  $\beta$ -actin. All IL-2-independent T-cell lines exhibited elevated MCT-1 protein levels in contrast to the IL-2-dependent T-cell lines, including IL-2-stimulated PBLs, which have low to undetectable MCT-1 protein levels.

## Results

### Elevated MCT-1 protein levels in exponentially growing T-lymphoid cell lines are not associated with point mutations

All IL-2-independent T-cell lines exhibited elevated MCT-1 protein levels. By contrast, the IL-2-dependent T-cell lines including IL-2-stimulated peripheral blood lymphocytes (PBLs) demonstrated low to absent MCT-1 protein levels (Figure 1). No amplification of the *MCT-1* gene was detected in any of these cell lines (data not shown). If the *MCT-1* gene is not amplified, the potential still exists for it to be activated through point mutations. The RT-PCR SSCP assay was used to screen for point mutations that may exist in the *MCT-1* gene. There was no altered migration of bands in any of the T-cell lines compared with the normal PBL samples (data not shown). Separation of the amplified coding region into 2 fragments smaller than 500 bp each greatly diminished the likelihood that we failed to detect point mutations under our assay conditions.<sup>11</sup>

### Steady-state MCT-1 protein levels in a panel of transformed B-cell lines derived from patients with non-Hodgkin lymphoma

This striking association of growth factor independence with elevated MCT-1 protein levels in T-cell lymphoid tumor lines prompted us to examine the expression of MCT-1 in other lymphoid malignancies. We studied a panel of lymphoma cell lines derived from patients with NHL. Most expressed high levels of MCT-1 protein when standardized to levels of  $\beta$ -actin protein (Figure 2).

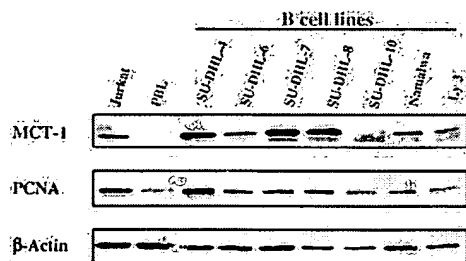


**Figure 2.** Steady-state MCT-1 protein levels in a panel of transformed B-cell lines derived from patients with non-Hodgkin lymphoma. Western blotting was performed with MCT-1 polyclonal antibody on 40  $\mu$ g total protein from 7 transformed B-cell lines. Results showed that most B-cell lines expressed high levels of MCT-1 protein and that MCT-1 levels are closely correlated with PCNA expressions in these cell lines. Jurkat and PBL cells served as positive and negative controls for MCT-1 signals, respectively.

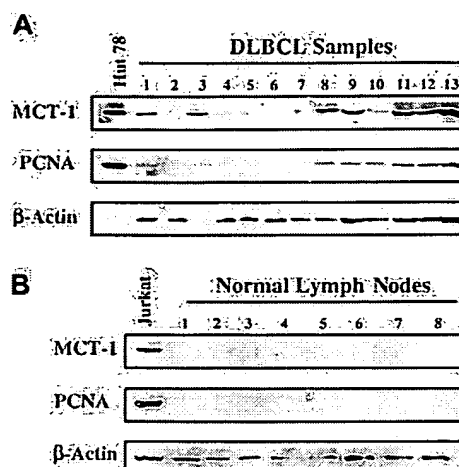


**Figure 3.** MCT-1 protein levels are increased in primary samples from a subset of patients. (A) Western blotting was carried out to detect MCT-1 and PCNA proteins from grossly involved lymph nodes of patients with newly diagnosed DLBCL. Seven of 13 specimens displayed elevated MCT-1 protein levels and were shown to correlate with increased PCNA levels. All 4 transformed lymphomas in our group demonstrated strong signals for MCT-1 protein (samples 3, 8, 9, and 11). (B) Ten normal lymph nodes examined had no detectable MCT-1 or PCNA. The Jurkat cell line served as a positive control for MCT-1 and PCNA protein expression.

### MCT-1 protein levels are increased in a subset of patients with DLBCL

Based on the results obtained from NHL cell lines, we proceeded to analyze primary lymphoma samples. We examined lymph node biopsy specimens obtained at initial diagnosis from patients with DLBCL. As shown in Figure 3A, 7 specimens displayed readily detectable MCT-1 protein. Positive findings were found in 7 of 17 (41%) NHL patients and in 0 of 10 (0%) control subjects (Figure 3B). This difference was statistically significant using Fisher exact test (41% vs 0%;  $P = .026$ ). All 4 transformed lymphomas in our group demonstrated strong signals for MCT-1 protein. Elevated MCT-1 protein levels were also shown to correlate with increased PCNA levels (Figure 3A-B).

### MCT-1 protein is not expressed in chronic lymphocytic leukemia

In primary uncultured samples ( $n = 10$ ) of B-cell chronic lymphocytic leukemia (CLL), we found low to undetectable levels of MCT-1 protein in the peripheral lymphocytes from untreated patients (Figure 4). These results are not unexpected because

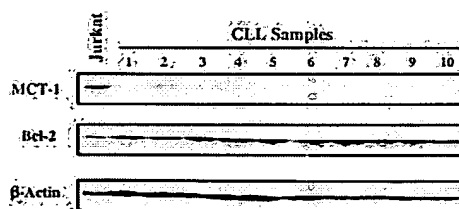


**Figure 4.** MCT-1 protein is not expressed in chronic lymphocytic leukemia. Western blotting was performed on 40  $\mu$ g whole cell lysate with MCT-1 polyclonal antibody. All samples were isolated from peripheral blood of untreated patients (with more than 80% lymphocytes). Protein from Jurkat cells was served as MCT-1-positive control. Control immunoblotting with  $\beta$ -actin verified equal loading. Bcl-2 protein was universally expressed in the patients we analyzed. Peripheral lymphocytes from primary uncultured B-CLL samples demonstrated low to undetectable levels of MCT-1 protein.

leukemic cells in this indolent lymphoid malignancy are primarily arrested in the G<sub>0</sub>/G<sub>1</sub> stage.<sup>12,13</sup>

### Overexpression of MCT-1 promotes cell proliferation

To examine the effect of constitutive overexpression of MCT-1 on cell-cycle progression of stably transfected lymphoid cell lines, we performed confocal microscopy on EC155-Vector<sup>5</sup> or EC155-MCT-1<sup>7</sup> cell lines. The EC155-MCT-1<sup>7</sup> cells showed a marked increase in the proportion of cells staining positively for PCNA, both by confocal analysis and by Western blot analysis (Figure 5).

We also observed a significant difference in the growth rate of MCT-1 overexpressing cells. The growth curve demonstrates the increased growth rate in 3 independent clones overexpressing MCT-1 compared with vector controls ( $P < .001$ ) (Figure 6A). MCT-1 overexpressing cells also demonstrate a higher percentage of cells in S-phase than do matched vector control cells, as shown by the increased level of PCNA protein staining (Figure 6B). These aggregate data support the role of MCT-1 in cell proliferation.

### EC155-MCT-1 cells survive in serum starvation

To investigate a possible role of MCT-1 in cell survival, the effect of serum deprivation was investigated. Serum deprivation resulted in significantly increased death in the vector controls than in the MCT-1 overexpressing clones. The viability of EC155-MCT-1 after 72-hour serum starvation is significantly higher than that of EC155-vector control ( $P < .01$ ), as determined by trypan blue dye exclusion (Figure 7).

### MCT-1 protein protects against apoptosis

To prove that cell death resulted from apoptosis, annexin V binding assays were performed. Annexin V binds to phosphatidylserine, a phospholipid that normally is present at the inner leaflet of the cell membrane but that, during apoptosis, is exposed at the outer leaflet. In the presence of serum, neither cell line significantly bound annexin V. However, after 48 to 72 hours of serum depletion, the EC155-Vector<sup>5</sup> cells heavily stained with annexin V-FITC, and EC155-MCT-1<sup>7</sup> cultures stained significantly less (Figure 8). The

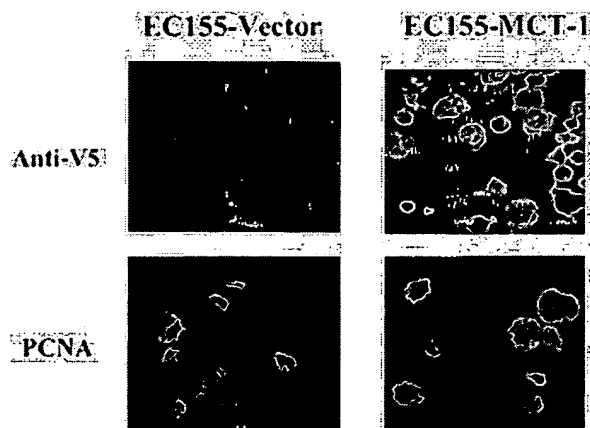


**Figure 5. Confocal immunofluorescence microscopy of EC155 cell lines.** EC155-Vector<sup>5</sup> and EC155-MCT-1<sup>7</sup> cells were fixed with methanol and incubated with blocking solution and primary antibody, mouse monoclonal anti-V5, or anti-PCNA. Next, secondary antimouse IgG2a-fluorescein was used for hybridization. Cells were spread on slides and mounted on coverglass with mounting medium. Slides were examined using a Zeiss LSM510 confocal scanning laser microscope. Results showed that MCT-1 overexpressing cells had elevated PCNA protein levels compared with control. Original magnification,  $\times 40$ .

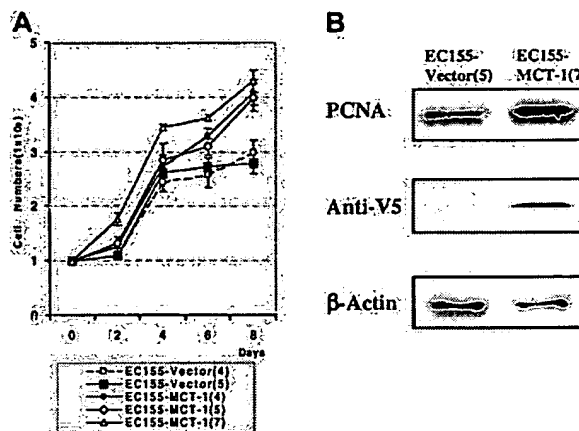


**Figure 6. MCT-1 overexpression increases the growth rate of lymphoid cells.** (A) EC155-Vector or EC155-MCT-1 cells were seeded at  $0.5 \times 10^6$  cells/mL in triplicate T-25 flasks. Cells were counted every other day by using the trypan blue exclusion method for 8 days. The growth curve demonstrated the significantly increased growth rate in EC155-MCT-1 clones. Data were derived from 3 independent experiments with each clone. Error bars denote mean  $\pm$  SD. (B) The EC155-MCT-1 cells showed a marked increase in PCNA level.

data presented are representative of the other clones as well. Another hallmark of early apoptosis is mitochondrial membrane permeabilization, which is regulated by numerous effectors, including the proteins from the Bcl-2/Bax family. We have observed the increase in mitochondrial membrane permeabilization after serum starvation occurring more frequently in the EC155-Vector<sup>5</sup> cell line than in the EC155-MCT-1<sup>7</sup> cell line (data not shown).

### MCT-1 enhances AKT phosphorylation at residue of Ser473

AKT plays a critical role in controlling the balance between cell survival and apoptosis.<sup>14</sup> This protein kinase is activated by growth/survival factors and is involved in phosphoinositide 3-kinase (PI3-kinase) signaling transduction. Akt is activated by PDK1-dependent phosphorylation at Thr308 and Ser473 residues.<sup>15,16</sup> The specific antibody against phospho-Ser473 on AKT was used to test EC155-Vector and EC155-MCT-1 cells (Figure 9).

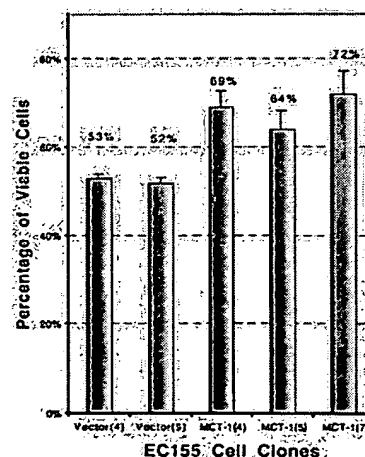


**Figure 7. MCT-1 promotes cell survival in serum-starvation culture.** EC155-Vector or EC155-MCT-1 cells ( $2 \times 10^6$  cells/mL) were seeded in triplicate wells in 12-well plates in serum-starved culture (0.2% FBS). Cell viability was analyzed by using the trypan blue exclusion method at certain time points. Data were presented as percentage of viable cells (mean  $\pm$  SD) and were derived from 3 independent experiments with each clone. The viability of EC155-MCT-1 after 72 hours of serum starvation was significantly higher than that of EC155-vector control.

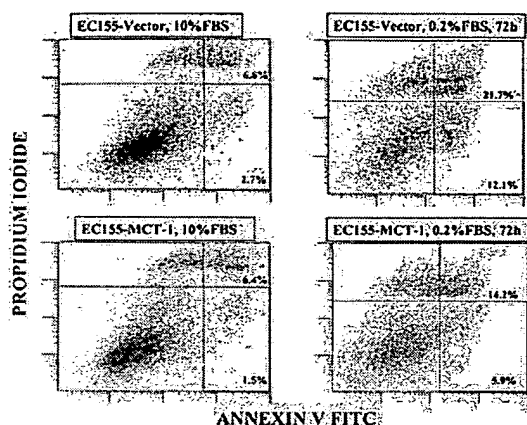


**Figure 8. MCT-1 protein protects against apoptosis.** Annexin V binding assay by flow cytometry was performed to compare cell apoptosis induction in EC155-Vector<sup>6</sup> and EC155-MCT-1<sup>7</sup> cell lines. After 72 hours of serum starvation, total annexin V-positive cells of the EC155-MCT-1<sup>7</sup> line was significantly less than that of EC155-Vector<sup>6</sup> (20.1% vs 33.8%). Similar results were obtained with other MCT-1 overexpressing clones. The data suggest a protective function of MCT-1 against apoptosis induced by serum starvation.

Our data revealed that phosphorylation level of AKT on Ser473 residue was significantly increased in MCT-1 overexpressing clones. Thus, MCT-1 may enhance AKT kinase activation to promote cell survival by inhibiting apoptosis.

## Discussion

The MCT-1 candidate oncogene product transforms fibroblasts and pushes them through the G<sub>1</sub>/S-phase of the cell cycle.<sup>3,17</sup> In the present study, we examined the expression status of the recently discovered candidate oncogene *MCT-1* in a diverse panel of primary lymphoid tumors and lymphoid cell lines. We also investigated the role of MCT-1 on cell growth and in protecting lymphoid cells against apoptosis. Our results demonstrated that MCT-1 protein expression was significantly elevated in some samples of aggressive lymphoma, including diffuse large B-cell lymphoma (DLBCL) and IL-2-independent T-cell lymphoid tumors. By contrast, chronic lymphocytic leukemia (CLL), an indolent lymphoproliferative disorder,<sup>12,13</sup> and the IL-2-dependent T-cell lines exhibited low to undetectable amounts of MCT-1 protein. We also observed a significant difference in the growth rate of MCT-1 overexpressing cells. Elevated MCT-1 protein levels were shown to strongly correlate with increased proliferating cell nuclear antigen (PCNA) levels. We showed that MCT-1 protein levels are associated with increased cell proliferation in human primary lymphoid tumors. Furthermore, we demonstrated that forced expression in lymphoid cell lines increased their proliferative rates using 2 independent assays, growth curve and PCNA staining. We detected no evidence of point mutations in the coding region of MCT-1 in those tumors with elevated levels of MCT-1 protein. The finding that elevated MCT-1 protein expression is more frequent in transformed lymphomas is consistent with our hypothesis that this candidate oncogene provides a growth advantage to lymphoma cells and may be associated with a more aggressive clinical course. It is possible that a minor population of normal lymphocytes expresses MCT-1 protein below our detection limit and that the primary DLBCL shown here may represent the *in vivo* transformation of relatively rare MCT-1-expressing normal B cells. Once MCT-1 antibodies that work on paraffin-embedded

tissues are available, we will be able to more critically address this issue and evaluate the relationship between MCT-1 protein levels and clinical parameters in a large study of DLBCL. The mechanism(s) of increased MCT-1 protein levels in a subset of human lymphoid tumors is unknown and is an area of active research in our laboratory.

The impact of decreased/increased MCT-1 protein levels on cell-cycle progression and protection against apoptosis in lymphoid tumors may shed new light on the physiological relevance of MCT-1. Given that cells that are deprived of essential growth factors normally undergo apoptosis, the inhibition of apoptosis is thought to be an important requirement in the process of oncogenesis. In view of the biologic relevance of apoptosis, we investigated whether the increased protection against cell death by MCT-1 *in vitro* was caused by an inhibition of apoptosis. Inhibition of apoptosis by MCT-1 would provide a physiological selective advantage *in vivo* for MCT-1-transformed cells. The trypan blue dye assay measures the number of surviving cells but does not distinguish between death by necrosis or apoptosis. We have shown by annexin V staining and mitochondrial membrane permeabilization that increased MCT-1 protein expression in lymphoid cells results in protection against apoptosis induced by serum starvation. The best-described antiapoptotic pathway is the PI3-kinase/Akt pathway. Generally, PKB/Akt activity is correlated with the phosphorylation of Ser473 and Thr308.<sup>15,16</sup> Under our experimental conditions, serum-starved EC155-MCT-1 cells and EC155-Vector cells contain similar amounts of total PKB/Akt protein. However, we found that with starvation, the SER(P) 473 PKB levels in EC155-MCT-1 cells are increased compared with EC155-Vector cells. Thus, the PKB/Akt phosphorylation levels in these cells correspond well with the differential resistance we observed against apoptosis induced by serum starvation. MCT-1 may function as a positive up-stream regulator of AKT, or MCT-1 could modulate Akt activity by inhibiting phosphatase activity, such as a tumor-suppressor PTEN. The molecular mechanism(s) underlying the antiapoptotic activity of MCT-1 and its putative involvement in PI3/AKT signaling pathway are under investigation. Our results suggest that the inhibition of apoptosis may be an important mechanism of MCT-1.

The demonstration that MCT-1 has *in vitro* transforming and antiapoptotic functions does not yet prove a primary role in lymphomagenesis. Additional experiments demonstrating transformation in whole animal studies are ongoing and are of critical

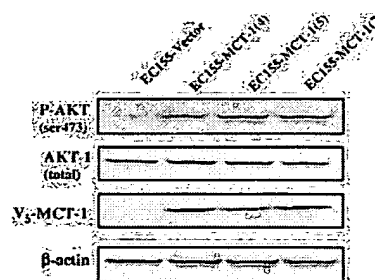


**Figure 9. MCT-1 overexpression enhances AKT phosphorylation at residue of Ser473.** Western blot analysis of extracts (150  $\mu$ g) was performed on EC155-Vector and EC155-MCT-1 cell lines. Nitrocellulose membranes were immunoblotted by anti-V5 after rehybridization with anti-phospho-AKT (Ser473), AKT, and actin antibodies after stripping overnight with 200 mM glycine (pH 2.5). The phosphorylation level of AKT on Ser473 residue was increased significantly in MCT-1 overexpressing cells compared with the vector control.

importance to address this issue. Although the underlying mechanisms are still unclear, others have found that molecular determinants predict outcome more accurately than clinical parameters<sup>18,19</sup> and that the identification of novel genes may result in models that can predict outcome. Indeed, investigators have shown that molecular profiling can segregate otherwise identical presentations of DLBCL into prognostic groups.<sup>20-22</sup> Molecular profiling may be able to predict outcome and to drive therapeutic decisions in these

patients and may prove to be complementary to the clinical prognostic factors in use today. The identification of novel genes that encode proteins, which confer a growth advantage to lymphoma cells, will help to clarify molecular profiling data. As the function of the *MCT-1* gene in regulating cell growth and apoptosis is further characterized, its putative role in lymphomagenesis will be elucidated. Ultimately, overexpressed or modified proteins may serve as targets for protein-specific therapy.

## References

- Gartenhaus RB. Microsatellite instability in hematologic malignancies. *Leuk Lymphoma*. 1997;25:455-461.
- Gamberi B, Gaidano G, Pansa N, et al. Microsatellite instability is rare in B-cell non-Hodgkin's lymphomas. *Blood*. 1997;89:975-979.
- Prosniak M, Dierov J, Okami K, et al. A novel candidate oncogene, MCT-1, is involved in cell cycle progression. *Cancer Res*. 1998;58:4233-4237.
- Monni O, Joensuu H, Franssila K, Knuutila S. DNA copy number changes in diffuse large B-cell lymphoma—comparative genomic hybridization study. *Blood*. 1996;87:5269-5278.
- Werner CA, Dohner H, Joos S, et al. High-level DNA amplifications are common genetic aberrations in B-cell neoplasms. *Am J Pathol*. 1997;15:335-342.
- Scarpa A, Taruscio D, Scardoni M, et al. Nonrandom chromosomal imbalances in primary mediastinal B-cell lymphoma detected by arbitrarily primed PCR fingerprinting. *Genes Chromosomes Cancer*. 1999;26:203-209.
- Herbert GB, Shi B, Gartenhaus RB. Expression and stabilization of the MCT-1 protein by DNA damaging agents. *Oncogene*. 2001;20:6777-6783.
- Berneman ZN, Gartenhaus RB, Reitz, et al. Expression of alternatively spliced human T-lymphotropic virus type I pX mRNA in infected cell lines and in primary uncultured cells from patients with adult T-cell leukemia/lymphoma and healthy carriers. *Proc Natl Acad Sci U S A*. 1992;89:3005-3009.
- Gartenhaus RB, Wong SF, Klotman ME. The promoter of human T-cell leukemia virus type-I is repressed by the immediate-early gene region of human cytomegalovirus in primary blood lymphocytes. *Blood*. 1991;78:2956-2961.
- Schlegel J, Vogt T, Munkel K, Ruschoff J. DNA fingerprinting of mammalian cell lines using non-radioactive arbitrarily primed PCR (AP-PCR). *Bio-techniques*. 1996;20:178-180.
- Gartenhaus RB, Wang P. Functional inactivation of wild-type p53 protein correlates with IL-2 independent growth of HTLV-I transformed human T-lymphocytes. *Leukemia*. 1995;9:2082-2086.
- Lagneaux L, Delforge A, Bernier M, Stryckmans P, Bron D. TGF-beta activity and expression of its receptors in B-cell chronic lymphocytic leukemia. *Leuk Lymphoma*. 1998;31:99-106.
- Cohen DP, Adams DJ, Flowers JL, et al. Pre-clinical evaluation of SN-38 and novel camptothecin analogs against human chronic B-cell lymphocytic leukemia lymphocytes. *Leuk Res*. 1999;23:1061-1070.
- Testa JR, Bellacosa A. AKT plays a central role in tumorigenesis. *Proc Natl Acad Sci U S A*. 2001;98:10983-10985.
- Alessi DR, Andjelkovic M, Caudwell B, et al. Mechanism of activation of protein kinase B by insulin and IGF-1. *EMBO J*. 1996;15:6541-6551.
- Kandel ES, Hay N. The regulation and activities of the multifunctional serine/threonine kinase Akt/PKB. *Exp Cell Res*. 1999;253:210-229.
- Dierov J, Prosniak M, Gallia G, Gartenhaus RB. Increased G1 cyclin/cdk activity in cells overexpressing the candidate oncogene, MCT-1. *J Cell Biochem*. 1999;74:544-550.
- Shipp MA, Ross KN, Tamayo P, et al. Diffuse large B-cell lymphoma outcome prediction by gene-expression profiling and supervised machine learning. *Nat Med*. 2002;8:68-74.
- Alizadeh AA, Eisen MB, Davis RE, et al. Distinct types of diffuse large B-cell lymphoma identified by gene expression profiling. *Nature*. 2000;403:503-511.
- Arber DA. Molecular diagnostic approach to non-Hodgkin's lymphoma. *J Mol Diagn*. 2000;2:178-190.
- Aguilar RC, Yakushijin Y, Kharbada S, Salgia R, Fletcher JA, Shipp MA. BAL is a novel risk-related gene in diffuse large B-cell lymphomas that enhances cellular migration. *Blood*. 2000;96:4328-4334.
- Hegde U, Wilson WH. Gene expression profiling of lymphomas. *Curr Oncol Rep*. 2001;3:243-249.



A service of the National Library of Medicine  
and the National Institutes of Health

My NCBI  
[Sign In] [Register]

All Databases PubMed Nucleotide Protein Genome Structure OMIM PMC Journals Books

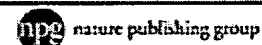
Search PubMed for

Limits Preview/Index History Clipboard Details

Display AbstractPlus  20

All: 1 Review: 0

☐ 1: Oncogene. 2005 Jul 21;24(31):4956-64.



Links

**The MCT-1 oncogene product impairs cell cycle checkpoint control and transforms human mammary epithelial cells.**

**Hsu HL, Shi B, Gartenhaus RB.**

Division of Hematology/Oncology, Department of Medicine, Northwestern University Feinberg School of Medicine and the Robert H Lurie Comprehensive Cancer Center of Northwestern University, Chicago, IL 60611, USA.

Multiple copies in T-cell malignancy (MCT-1) is a putative oncogene initially identified in a human T-cell lymphoma. Forced expression of MCT-1 has recently been shown to induce cell transformation and proliferation, as well as to activate survival-related PI-3K/AKT pathways protecting cells from apoptosis. MCT-1 protein is stabilized in response to DNA damage. The impact of MCT-1 overexpression on DNA damage response remains unknown. Here, we show that MCT-1 deregulates cell cycle checkpoints. The phosphorylation of genomic stabilizers H2AX and NBS1 are enhanced in MCT-1-overexpressing cells. Forced expression of MCT-1 significantly increases the number of DNA damage-induced foci involving gamma-H2AX and 53BP1. In MCT-1-overexpressing cells, the proportion of S-phase cell population is preferentially increased after exposure to gamma-irradiation compared to controls. Knockdown of endogenous MCT-1 using an siRNA approach attenuates the H2AX phosphorylation and the G1/S checkpoint defect. Furthermore, MCT-1 is capable of transforming immortalized human mammary epithelial cells and promoting genomic instability. These data shed light on the role of MCT-1 in the cellular response to DNA damage and its involvement in malignant transformation.

PMID: 15897892 [PubMed - indexed for MEDLINE]

**Related Links**

Expression and stabilization of the MCT-1 protein by DNA damaging agents. [Oncogene. 2001]

Overexpression of c-Myc alters G (1)/S arrest following ionizing radiation. [Mol Cell Biol. 2002]

Expression of the candidate MCT-1 oncogene in B- and T-cell lymphoid malignancies. [Blood. 2003]

A novel candidate oncogene, MCT-1, is involved in cell cycle progression. [Cancer Res. 1998]

Assessment of ATM phosphorylation on Ser-1981 induced by DNA topoisomerase I and II inhibitors in relation to Ser-139-histone H2AX phosphorylation, cell cycle phase, and apoptosis. [Cytometry A. 2005]

See all Related Articles...

Display AbstractPlus  20

[Write to the Help Desk](#)

[NCBI](#) | [NLM](#) | [NIH](#)

Department of Health & Human Services

[Privacy Statement](#) | [Freedom of Information Act](#) | [Disclaimer](#)

**This Page is Inserted by IFW Indexing and Scanning  
Operations and is not part of the Official Record**

**BEST AVAILABLE IMAGES**

Defective images within this document are accurate representations of the original documents submitted by the applicant.

Defects in the images include but are not limited to the items checked:

- ☐ BLACK BORDERS
- ☐ IMAGE CUT OFF AT TOP, BOTTOM OR SIDES
- ☒ FADED TEXT OR DRAWING
- ☐ BLURRED OR ILLEGIBLE TEXT OR DRAWING
- ☐ SKEWED/SLANTED IMAGES
- ☐ COLOR OR BLACK AND WHITE PHOTOGRAPHS
- ☐ GRAY SCALE DOCUMENTS
- ☐ LINES OR MARKS ON ORIGINAL DOCUMENT
- ☐ REFERENCE(S) OR EXHIBIT(S) SUBMITTED ARE POOR QUALITY
- ☐ OTHER: \_\_\_\_\_

**IMAGES ARE BEST AVAILABLE COPY.**

**As rescanning these documents will not correct the image problems checked, please do not report these problems to the IFW Image Problem Mailbox.**